Open Access Full Text Article

ORIGINAL RESEARCH

Papaverine inhibits lipopolysaccharide-induced microglial activation by suppressing NF-κB signaling pathway

Yalong Dang[1]
Yalin Mu[2]
Kun Wang[3]
Ke Xu[2]
Jing Yang[1]
Yu Zhu[1]
Bin Luo[2,3]

[1]Department of Ophthalmology, The First Affiliated Hospital of Zhengzhou University, Zhengzhou, People's Republic of China; [2]Department of Ophthalmology, Yellow-River Hospital, Sanmenxia City, People's Republic of China; [3]Clinical Laboratory, Yellow-River Hospital, Sanmenxia City, People's Republic of China

Correspondence: Yu Zhu
Department of Ophthalmology, The First Affiliated Hospital of Zhengzhou University, East Jianshe Road, 450001 Zhengzhou, People's Republic of China
Email asiadragon@163.com

Bin Luo
Department of Ophthalmology, Yellow-River Hospital, West Heping Road, Hubin District, 472000 Sanmenxia City, People's Republic of China
Email 13569610688@126.com

Objective: To investigate the effects of papaverine (PAP) on lipopolysaccharide (LPS)-induced microglial activation and its possible mechanisms.

Materials and methods: BV2 microglial cells were first pretreated with PAP (0, 0.4, 2, 10, and 50 μg/mL) and then received LPS stimulation. Transcription and production of proinflammatory factors (IL1β, TNFα, iNOS, and COX-2) were used to evaluate microglial activation. The transcriptional changes undergone by M1/M2a/M2b markers were used to evaluate phenotype transformation of BV2 cells. Immunofluorescent staining and Western blot were used to detect the location and expression of P65 and p-IKK in the presence or absence of PAP pretreatment.

Results: Pretreatment with PAP significantly inhibited the expression of IL1β and TNFα, and suppressed the transcription of M1/M2b markers Il1rn, Socs3, Nos2 and Ptgs2, but upregulated the transcription of M2a markers (Arg1 and Mrc1) in a dose-dependent manner. In addition, PAP pretreatment significantly decreased the expression of p-IKK and inhibited the nuclear translocation of P65 after LPS stimulation.

Conclusion: PAP not only suppressed the LPS-induced microglial activity by inhibiting transcription/production of proinflammatory factors, but also promoted the transformation of activated BV2 cells from cytotoxic phenotypes (M1/M2b) to a neuroprotective phenotype (M2a). These effects were probably mediated by NF-κB signaling pathway. Thus, it would be a promising candidate for the treatment of neurodegenerative diseases.

Keywords: papaverine, microglia, neuroprotection, neuroinflammation

Introduction

Microglial cells, representing 10%–20% of the total glial cells in the central nervous system (CNS), are the prime innate immunocytes responding against inflammatory, infectious, and other pathophysiological stimuli.[1] Under "rest" conditions, they show highly ramified shapes and actively supervise the microenvironment of CNS.[2] In case of acute insults, they quickly transform into highly activated ameboid-like shapes, phagocytize the injured neurons, release inflammatory factors, and thus restore the homeostasis of CNS.[3] However, if the insults cannot be controlled effectively, a chronic, self-propagating microglial response characterized by sustained release of cytotoxic molecules (cytokines, chemokines, and radical species) will be incurred,[4,5] which usually results in chronic neuroinflammation and secondary neuronal injury. This is a common phenomenon also observed in many acute/chronic retinal degenerative diseases, such as glaucoma,[6] age-related macular degeneration,[7] and ocular traumatic injury.[8] Therefore, inhibiting overactivated microglial responses and alleviating the

release of neurotoxic molecules are promising therapeutic approaches for these diseases.

To date, great efforts in screening new drugs capable of inhibiting overactivated microglial responses have achieved many progresses. Our team identified a set of drugs that exhibited anti-neuroinflammatory effects. We found that minocycline not only significantly decreased the number of activated microglia in the subretinal space and outer nuclear layer, but also remarkably alleviated the loss of photoreceptors in light-induced retinal degeneration.[9] Additionally, we also investigated the effects of tetrandrine on microglial activation and neural survival. We found 1 µM of tetrandrine significantly inhibited the production of TNFα and IL1β in mouse microglial cells[10], and alleviated the death of retinal ganglion cells in an acute ocular hypertension model.[11] However, since the working concentration of tetrandrine in vitro is much higher than that in the blood, it is hard to be used as an anti-neuroinflammatory drug in clinical practice.

Recently, we found papaverine (PAP), an isoquinoline alkaloid extracted from *Papaver somniferum* L, not only suppressed the lipopolysaccharide (LPS)-induced microglial activity by inhibiting transcription/production of proinflammatory factors, but also promoted the transformation of activated BV2 cells from cytotoxic phenotypes (M1/M2b) to a neuroprotective phenotype (M2a), and these effects were mediated by NF-κB signaling pathway.

Materials and methods
Ethics statement
All experiments were performed in accordance with the guidelines of Association for Research in Vision and Ophthalmology Statement and were approved by the Institutional Review Board of Zhengzhou University.

Study design
Cell viability assay was performed to determine the working concentrations of PAP (H32020967, Heng Rui Medicine Co. LTD, Jiangsu, People's Republic of China).

To evaluate the effects of PAP on microglial activation, BV2 cells were seeded on six-well plates overnight and pretreated with PAP at working concentration for 4 hours. Then, LPS (Sigma-Aldrich, St Louis, MO, USA; final concentration: 100 ng/mL) was added to the medium and continually incubated for 24 hours. The supernatant was collected for enzyme-linked immunosorbent assay (ELISA). The cells were lysed for real-time polymerase chain reaction (PCR) assay.

To investigate the possible mechanism involved in the action of PAP, the cells were seeded on poly-L-lysine coated dishes and pretreated with PAP as described earlier. Then, LPS was supplemented for another 1 hour. For immunofluorescence analysis, cells were fixed with 4% paraformaldehyde. For Western blotting, cells were lysed and the protein was extracted for further analysis.

Cell culture
Mouse BV2 microglial cells, purchased from the Cell Resource Center of Peking Union Medical University (Beijing, People's Republic of China), were maintained in Dulbecco's Modified Eagle's Medium (DMEM)/high glucose supplemented with 10% heat-inactivated FBS (fetal bovine serum) in a humidified incubator under 95%/5% (v/v) mixture of air and CO_2 at 37°C. Cells were digested and passaged at 80% confluence.

Cell viability assay
Cell viability was measured by Cell Counting Kit 8 (CCK-8, Dojindo Laboratories, Dalian, People's Republic of China) according to the manufacturer's instructions. Briefly, 100 µL of cells (3×10^4 cells/mL) was seeded into 96-well plates and incubated overnight. The medium was changed in the presence of PAP at different concentrations (0, 0.4, 2, 10, and 50 µg/mL) and incubated for 4 hours; then LPS final concentration of 100 ng/mL was added and continually incubated for another 24 hours. Ten microliters of CCK-8 solution was added to each well and incubated for 2 hours. Optical density was measured at 450 nm using a microplate reader (Sunrise, Tecan, Switzerland).

Reverse-transcriptase polymerase chain reaction (RT-PCR)
BV2 cells were prepared as described in the section "Study design". Then, the cells were lysed and total RNA was extracted by TRIzol Reagent (15596-026, Thermo Fisher Scientific, Waltham, MA, USA). RT-PCR and quantitative PCR were performed on the SuperScript One-Step RT-PCR System (AB7500, Thermo Fisher Scientific) according to the manufacturer's instructions. Briefly, ~1,000 ng of RNA template was reverse-transcribed using a PrimeScript™ RT Master Mix Kit (RR036A, TaKaRa Bio Inc, Dalian, People's Republic of China). Subsequently, 2 µL of cDNA solution of each sample was subjected to RT-PCR in a 20 µL reaction mixture containing 10 µL of 2× SYBR® Premix Ex Taq II, 0.4 µL of 50× ROX Reference Dye, 1.6 µL of PCR forward/reverse primer mixture (final concentration: 0.4 µM), and 6 µL of dH₂O; β-actin served as an internal control. The primers were designed as listed in Table 1.

Table 1 The primers for quantitative RT-PCR

Gene	Encoded protein	Forward primer 5'-3'	Reverse primer 5'-3'	Accession	Size (bp)
Il1b	IL1β	AATGACCTGTTCTTTGAAGTTGA	TGATGTGCTGCTGCGAGATTTGAAG	XM_006498795.1	115
Tnf	TNFα	GAAAAGCAAGCAGCCAACCA	CGGATCATGCTTTCTGTGCTC	NM_001278601.1	106
Nos2	iNOS	GAAGAAAACCCCTTGTGCTG	GTCGATGTCACATGCAGCTT	NM_010927.3	138
Ptgs2	COX2	GATGTTTGCATTCTTTGCCC	GGCGCAGTTTATGTTGTCTG	NM_011198.3	149
Mrc1	CD206	CTTCGGGCCTTTGGAATA	TAGAAGAGCCCTTGGGTTGA	NM_008625.2	150
Arg1	Arg1	GTGAAGAACCCACGGTCTGT	GCCAGAGATGCTTCCAACTG	NM_007482.3	132
Tgfb1	TGFb	CTTTTGACGTCACTGGAG	CAGTGAGCGCTGAATCGAA	NM_011577.1	79
Il1rn	IL-1ra	TTGTGCCAAGTCTGGAGA	TTCTCAGAGCGGATGAAGGT	XM_006497727.1	111
Socs3	SOCS3	CGTTGACAGTCTTCCGAC	TATTCTGGGGGCGAGAAGAT	XM_011248707.1	94
Actb	β-actin	TCCTCCTGAGCGCAAGTACTCT	GCTCAGTAACAGTCCGCCTAGAA	NM_007393.3	130

Abbreviation: RT-PCR, reverse transcriptase polymerase chain reaction.

ELISA

The supernatant was collected as described in the section "Study design". The production of IL1β and TNFα was measured by ELISA. Mouse IL1β ELISA kit (ab100705) and TNFα ELISA kit (ab100747) were purchased from Abcam Inc. (Cambridge, MA, USA). The experiments were conducted in accordance with the manufacturer's instructions.

Western blot analysis

Total proteins were prepared using RIPA lysis buffer (Sigma-Aldrich) supplemented with 1 mM phenylmethanesulfonylfluoride (PMSF, Sigma-Aldrich). Nuclear proteins were extracted using Nuclear and Cytoplasmic Protein Extraction Kit (P0028, Beyotime, Shanghai, People's Republic of China). After centrifugation at $12,000 \times g$ for 15 minutes at 4°C, the supernatant was collected and protein concentration was determined by a Bicinchoninic Acid Protein Assay Kit (BD0028, Bioworld, Dublin, OH, USA). Approximately, 30 μg of protein sample was loaded into each well of a 10% SDS-PAGE gel for electrophoresis, followed by electrotransfer to polyvinylidenedifluoride membranes (GE Healthcare, Beijing, People's Republic of China). The membranes were blocked prior to incubation with primary antibodies, NF-κB P65 (C22B4) rabbit mAb (1:1,000; #4764, Cell Signaling, Danvers, MA, USA), Phospho-IKK α/β (Ser176/180) (16A6) rabbit mAb (1:1,000; #2697, Cell Signaling), β-actin (1:500; #ab3280, Abcam), and Lamin B (1:1,000; Santa Cruz Biotechnology Inc., Dallas, TX, USA, a kind gift from Dr Zhang), overnight at 4°C. After washing with phosphate-buffered saline (PBS) for three times, the membrane was incubated with horseradish peroxidase (HRP)-conjugated secondary antibody (1:1,000; A0208, Beyotime), developed with Super signal West Dura Extended Duration Substrate (Thermo Scientific Pierce, Rockford, IL, USA), and imaged using an Autochemie System (UVP, Upland, CA, USA). The

relative expression of p-IKK and nuclear P65 was normalized with β-actin and Lamin B, respectively.

Immunofluorescent staining

Cells were fixed with 4% paraformaldehyde for 10 minutes, then permeabilized and blocked with Immunol Staining Blocking Buffer (P0102, Beyotime) for 45 minutes at room temperature. Cells were incubated with NF-κB P65 (C22B4) rabbit mAb (1:100; #4764, Cell Signaling) or Phospho-IKK α/β (Ser176/180) (16A6) rabbit mAb (1:150; #2697, Cell Signaling) overnight at 4°C. After three washes with PBS, 50 μL of Goat anti-rabbit IgG H&L (Alexa Fluor® 488) secondary antibody (1:1,000; ab150077, Abcam) was added and incubated for 2 hours at room temperature. Diamidino-phenyl-indole (DAPI) was used to label the nuclei. Finally, images were captured by a fluorescence microscope.

Statistical analyses

Results were represented as the mean ± SD (standard deviation). The statistical significance of differences was compared by one-way analysis of variance followed by Dunnett's test. Two-tailed values of $P < 0.05$ were considered to be statistically significant.

Results

Noncytotoxic effects of PAP under proper concentrations

In this study, cell viability test (CCK-8 assay) was used to evaluate the cytotoxic effects of PAP on BV2 cells. As shown in Figure 1, compared with the control group, pretreatment with 50 μg/mL of PAP significantly inhibited the viability of BV2 cells ($P < 0.05$), while no significant difference was observed for the concentrations below 10 μg/mL ($P > 0.05$). Therefore, PAP at a concentration range from 0 to 10 μg/mL was used in the following experiments.
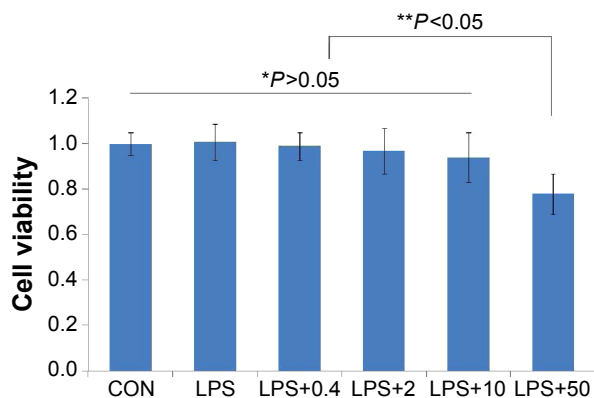
Figure 1 The effects of PAP on the viability of BV2 cell.
Notes: BV2 cells were pretreated with PAP (0, 0.4, 2, 10, and 50 μg/mL) for 4 hours followed by LPS (100 ng/mL) stimulation for an additional 24 hours. Cell viability was measured by CCK-8 assay. Compared with the control group, pretreatment with 50 μg/mL of PAP significantly inhibited the cell viability (**$P<0.05$), while no significant difference was observed at the concentrations below 10 μg/mL (*$P>0.05$). The results are represented as the mean ± SD of three independent experiments.
Abbreviations: PAP, papaverine; LPS, lipopolysaccharide; CCK-8, Cell Counting Kit 8; SD, standard deviation; CON, control.

PAP suppressed LPS-induced microglial activation

BV2 cells are sensitive to LPS stimulation. In this study, the transcription and production of proinflammatory factors were utilized to evaluate microglial activation.

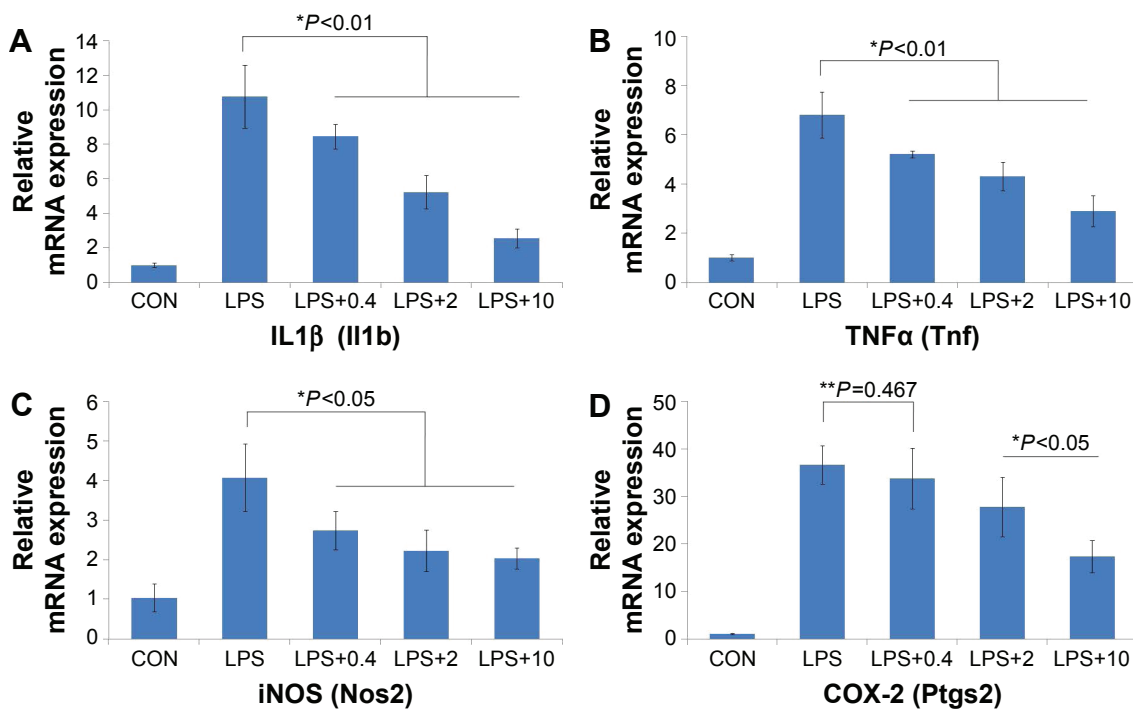## PAP inhibited the transcription of proinflammatory genes in a dose-dependent manner

The transcription of proinflammatory genes (Il1b, Tnf, Nos2, and Ptgs2) was measured by RT-PCR. As shown in Figure 2, LPS stimulation significantly increased the transcription of proinflammatory genes, while PAP pretreatment remarkably reversed these effects in a dose-dependent manner ($P<0.05$). Remarkably, pretreatment with 0.4 μg/mL of PAP was unable to suppress the transcription of Ptgs2 after LPS stimulation ($P=0.467$).

PAP attenuated the production of IL1β and TNFα in a dose-dependent manner

Consistent with the changes in transcription of Il1b (IL1β) and Tnf (TNFα), LPS stimulation significantly increased the production of IL1β and TNFα, while PAP pretreatment remarkably suppressed these effects in a dose-dependent manner ($P<0.001$, Figure 3).

## PAP modulated the phenotype transformation of BV2 cells

Generally, in response to stimulations, microglial cells are capable of acquiring four complex phenotypes: M1, M2a,

Figure 2 The transcription of proinflammatory genes after PAP pretreatment.
Notes: BV2 cells were pretreated with PAP (0, 0.4, 2, and 10 μg/mL) for 4 hours and received LPS stimulation for another 24 hours. Then total RNA was extracted for RT-PCR. (**A–D**) Shows the transcription of IL1β, TNFα, iNOS, and COX-2, respectively. LPS stimulation significantly increased the transcription of proinflammatory genes, while PAP pretreatment remarkably reversed these effects in a dose-dependent manner (*$P<0.05$). Remarkably, 0.4 μg/mL of PAP pretreatment was unable to suppress the transcription of COX-2 after LPS stimulation (**$P=0.467$). The results are represented as the mean ± SD of three independent experiments.
Abbreviations: PAP, papaverine; LPS, lipopolysaccharide; RT-PCR, reverse transcriptase polymerase chain reaction; SD, standard deviation; CON, control.

A

B
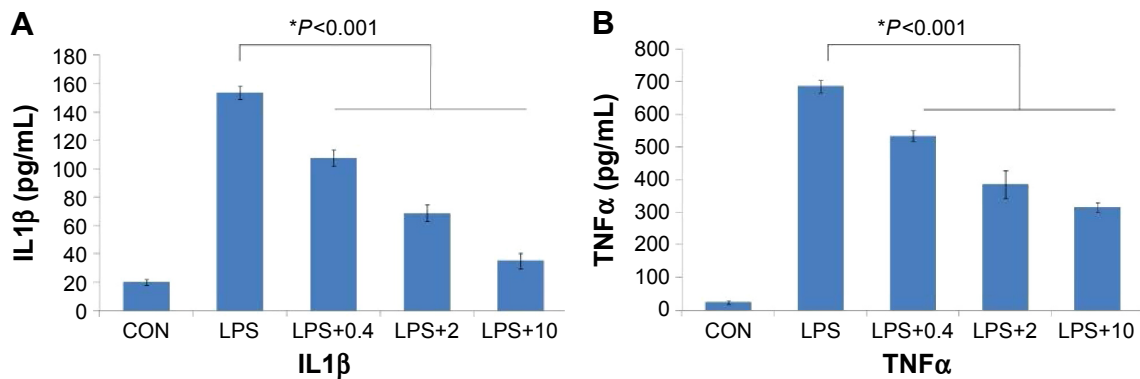
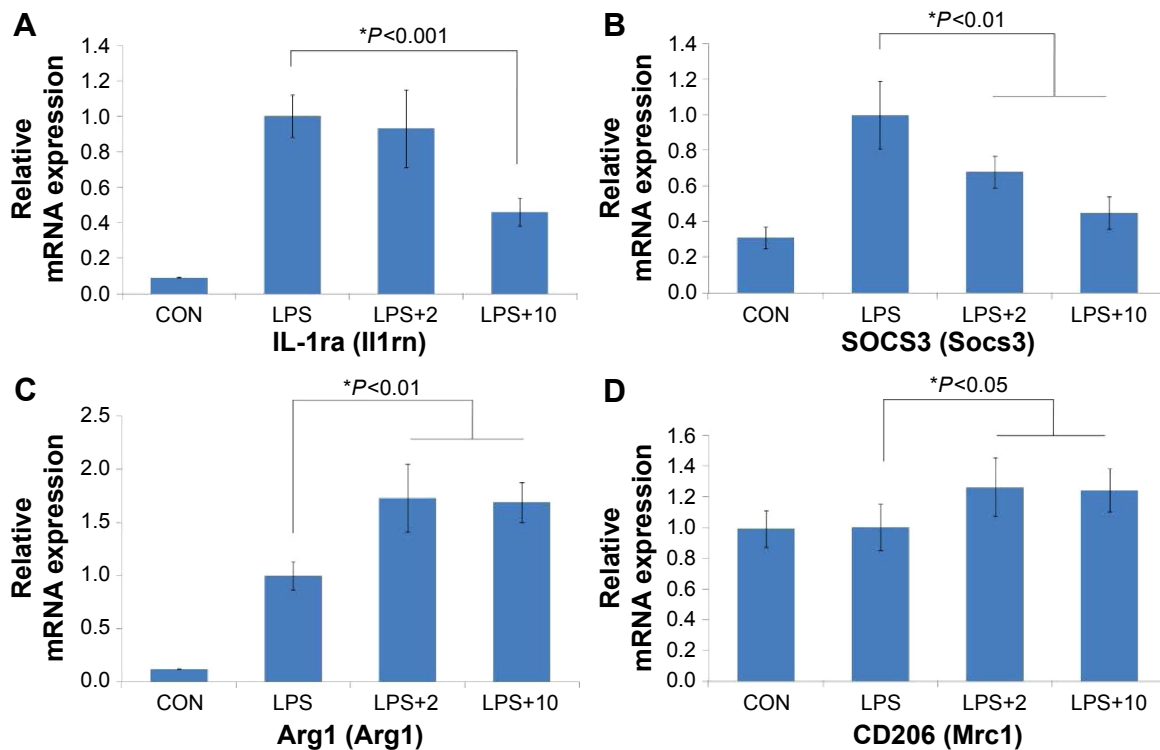**Figure 3** The production of IL1β and TNFα after PAP pretreatment.
Notes: Cells were pretreated with PAP (0, 0.4, 2, and 10 μg/mL) for 4 hours and incubated with LPS (100 ng/mL) for an additional 24 hours. The production of IL1β and TNFα was measured by ELISA. PAP pretreatment remarkably inhibited the production of IL1β (**A**) and TNFα (**B**) in a dose-dependent manner (*P<0.001). The results are represented as the mean ± SD of three independent experiments.
Abbreviations: PAP, papaverine; LPS, lipopolysaccharide; ELISA, enzyme-linked immunosorbent assay; SD, standard deviation; CON, control.

M2b, and M2c. Figure 4 shows that PAP pretreatment significantly suppressed the transcription of M2b-associated markers (Il1rn and Socs3, $P<0.001$ and $P<0.01$, respectively), but upregulated the transcription of M2a-associated markers (Arg1 and Mrc1, $P<0.01$ and $P<0.05$, respectively). In addition, as demonstrated in Figure 2C and D, M1-associated markers (Nos2 and Ptgs2) were also downregulated after the PAP pretreatment.

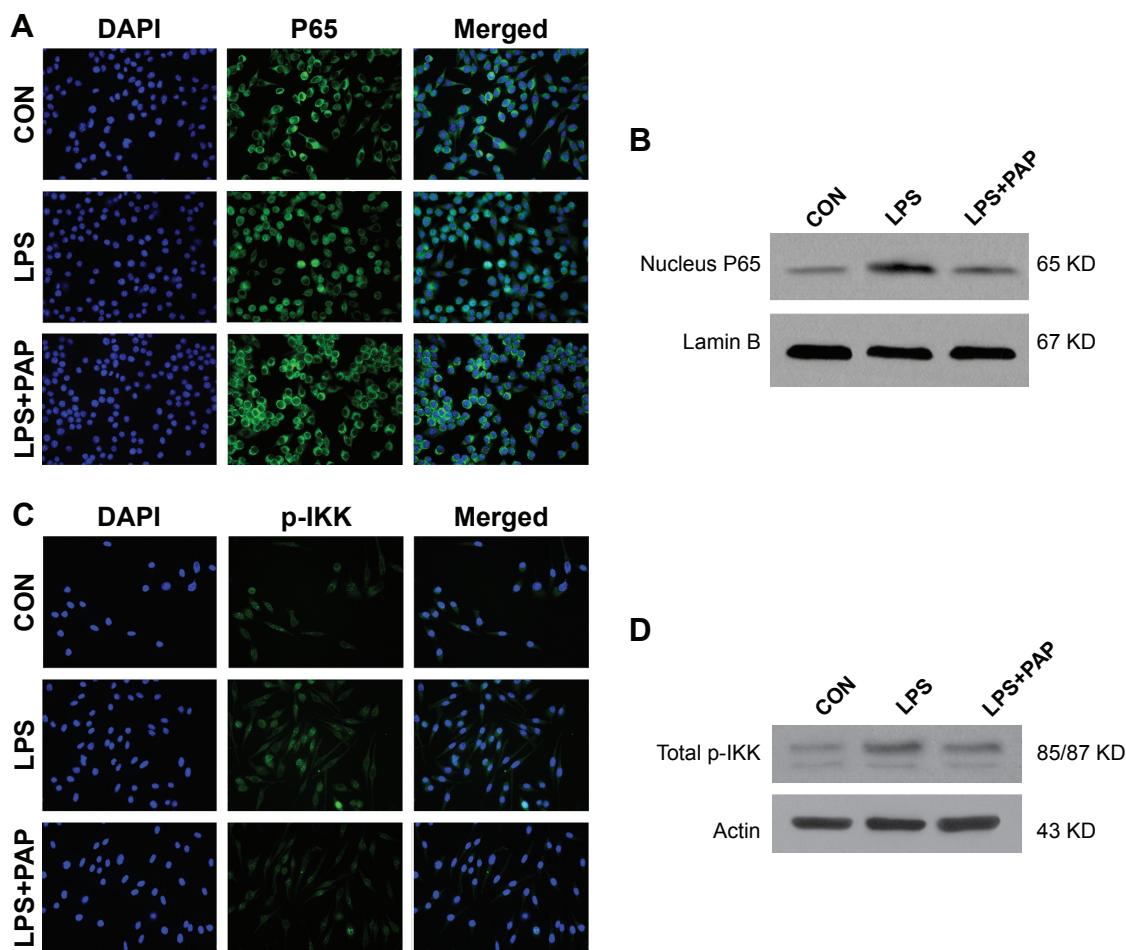## PAP suppressed LPS-induced microglial activation by NF-κB signaling pathway

NF-κB signaling pathway plays a vital role in inflammatory responses by regulating a set of genes encoding proinflammatory cytokines, that is, chemokines. NF-κB signaling is activated by the phosphorylation of IKK, which promotes the degradation of I-kB from NF-κB dimer. Then, NF-κB P65 could translocate to the nucleus and activate the target genes.

Figure 4 PAP modulated microglial phenotype transformation.
Notes: Cells were pretreated with PAP (0, 2, and 10 μg/mL) for 4 hours and incubated with LPS (100 ng/mL) for an additional 24 hours. The transcription of IL-1ra (Il1rn), SOCS3 (Socs3), Arg1 (Arg1), and CD206 (Mrc1) was measured by RT-PCR. (**A** and **B**) Shows PAP pretreatment significantly inhibited the transcription of M2b-associated markers IL-1ra (Il1rn), SOCS3 (Socs3) *P<0.01, but upregulated the transcription of M2a-associated markers Arg1 (Arg1) and CD206 (Mrc1) (**C** and **D**) *P<0.05. The results are represented as the mean ± SD of three independent experiments.
Abbreviations: PAP, papaverine; LPS, lipopolysaccharide; RT-PCR, reverse transcriptase polymerase chain reaction; SD, standard deviation; CON, control.

Figure 5 PAP suppressed LPS-induced microglial activation by NF-κB signaling pathway.
Notes: Cells were seeded on poly-L-lysine coated dishes and pretreated with PAP (10 μg/mL) for 4 hours. Then, LPS was added to the medium and incubated for another 1 hour. For immunofluorescence analysis, cells were fixed and incubated with primary/secondary antibodies. For Western blotting, cells were lysed and the total/nuclear protein was extracted for further analysis. A significant increase in nuclear translocation of P65 and remarkable upregulation of intranuclear P65 were noticed after 1 hour of LPS application, but this effect was partly abolished by 4 hours of PAP pretreatment (**A** and **B**). Consistent with the changes of P65, LPS stimulation increased phosphorylation of IKK in BV2 cells, but it was partly blocked by PAP pretreatment (**C** and **D**).
Abbreviations: PAP, papaverine; LPS, lipopolysaccharide; CON, control; DAPI, diamidino-phenyl-indole.

As shown in Figure 5A and B, we observed a significant increase in the nuclear translocation of P65 and a remarkable increase in the upregulation of intranuclear P65 after 1 hour of LPS application, but this effect was significantly abolished by pretreatment with 10 μg/mL of PAP for 4 hours. Consistent with the changes exhibited by P65, LPS stimulation increased phosphorylation of IKK in BV2 cells, but this was partly blocked by PAP pretreatment (Figure 5C and D).

In this study, we also tried to determine the role of MAPKs and p-STAT3 in LPS-induced microglial activation in the presence or absence of PAP pretreatment, but did not get a positive result (data not shown).

Discussion

Glaucoma, a neurodegenerative disease characterized by sustained loss of retinal ganglion cells (RGCs) and visual field,

is the leading cause of irreversible blindness worldwide.[12] Microglial activation plays a crucial role in the development of glaucomatous optic neuropathy.[6] Numerous evidences suggested that microglial activation takes place prior to the loss of RGCs[13] and that activated microglia are found clustered in the optic nerve head – the site of initial axonal degeneration.[14] Therefore, inhibiting microglial activation is a promising approach for glaucoma therapy. In this study, we identified PAP could significantly suppress the transcription and production of proinflammatory factors and modulate the phenotype transformation of BV cells (from M1/M2b to M2a). These effects are probably mediated by NF-κB signaling pathway. As a vasodilating agent, PAP is widely used in the treatment of visceral spasm and vasospasm.[15,16] The blood concentration (0.408 and 2.4 μg/mL after oral and intravenous administration, respectively) was similar to the

working concentrations used in this study.[17] Therefore, PAP might be a valuable anti-neuroinflammatory candidate for the treatment of neurodegenerative diseases.

Immortalized mouse cell line (BV2) was utilized to evaluate the microglial activation. This is mainly due to the reason that primary microglia obtained by the current protocols show decreased efficiency and that freshly isolated primary microglia exhibit similar morphological, functional, and phenotypical properties. Indeed, we were also able to detect the morphological changes of BV2 cells after LPS stimulation. In the presence of LPS (100 ng/mL), the BV2 cells quickly changed from spindle- or bipolar-like shapes to amoeboid-like shapes with short thick processes, but this condition could be reversed by pretreatment with 10 μg/mL of PAP (data not shown). Interestingly, in another study, we found PAP was unable to reverse the morphological changes of rat primary microglia induced by LPS.[18] These results suggested that although morphological changes and microglial activation are closely related, they might be mediated by different signaling pathways and that some differences exist between the species. However, the morphological changes are relatively less specific and sensitive in evaluating microglial activation. We evaluated the transcription and production of proinflammatory factors of BV2 cells after LPS stimulation. TNFα is a proinflammatory cytokine modulating the direct and secondary neurodegenerative injury in the CNS. There are several evidences that support the role of TNFα as a mediator of neurodegeneration in glaucomatous eyes.[19–21] Overexpression of TNFα after CNS injury has been associated with deterioration in neuronal damage, whereas its inhibition was correlated with a good outcome.[22,23] Su et al showed that inhibition of NF-κB signaling pathway by rapamycin not only suppressed the release of neurotoxic factors, but also decreased the apoptosis of RGCs in vitro and in vivo.[24] Yang et al also reported that improvement in the survival of RGCs could be obtained by modulating NF-κB pathway in a mouse glaucoma model.[25] IL1β, mainly produced by activated monocytes (including microglia), is another mediator in neuroinflammatory response. Recent studies suggested upregulation of IL1β was highly associated with some neurodegenerative diseases, such as glaucoma[26] and multiple sclerosis.[27] Mookherjee et al found that genomic region containing the IL1 gene cluster influenced the pathogenesis of normal-tension glaucoma.[26] A previous study also showed that IL1β at high doses could elevate the transcription of iNOS (Nos2) and thus increase NO production.[28] In this study, we found LPS stimulation significantly increased

the transcription of IL1β (Il1b), TNFα (Tnf), iNOS (Nos2), and COX-2 (Ptgs2), while PAP pretreatment remarkably reversed these effects in a dose-dependent manner. Consistent with the changes in gene transcription, the production of IL1β and TNFα was also decreased after the PAP pretreatment. Therefore, we concluded that PAP at proper concentrations could inhibit the expression of proinflammatory factors and alleviate neuroinflammatory response, and thus may be used to alleviate the neuronal damage in neurodegenerative diseases.

However, activated microglia acts multiple facets during neuroinflammation, not only cytotoxicity[29] but also neuroprotection.[30] The different biological effects exhibited by activated microglia are mainly attributed to the ability to transform into four diverse activation states:[31] M1 with cytotoxic properties; M2a with an alternate activation and involved in neuroprotection and regeneration; M2b with an immunoregulatory phenotype; and M2c with an acquired-deactivating phenotype. M1 and M2b mediate the primary and secondary neuronal injury, respectively, while M2a shows a negative effect. Therefore, modulation of microglial phenotype may represent an innovative strategy for the treatment of neurodegenerative diseases. In our study, we found that LPS stimulation significantly increased the transcription of M1 markers, such as iNOS (Nos2) and COX-2 (Ptgs2). PAP pretreatment remarkably suppressed the transcription of M2b markers (IL-1ra (Il1rn) and SOCS3 (Socs3)) and M1 markers (iNOS (Nos2) and COX-2 (Ptgs2)), but significantly upregulated the transcription of M2a markers (Arg1 (Arg1) and CD206 (Mrc1)) in a dose-dependent manner. The phenotype transformation induced by PAP indicates that it would be an ideal neuroprotectant in neurodegenerative diseases.

As PAP is a phosphodiesterase inhibitor, the anti-inflammatory effect of PAP may be attributed to the elevation in the levels of cAMP. Elevation of intracellular cAMP results in PKA activation and phosphorylation of CREB, and thus promotes the recruitment of coactivators, such as CREB or the homologous protein p300, away from NF-κB in the nucleus and finally inhibits the NF-κB signaling pathway.[32] However, we failed to observe any positive results associated with the changes in p-CREB after PAP pretreatment in BV2 cells (data not shown). We then evaluated the changes exhibited by P65 in the nucleus, p-IKK, p-ERK, p-38, and p-STAT3 in the presence or absence of PAP pretreatment, and found a prominent nuclear translocation of P65 after LPS application, but PAP significantly reversed this effect. In addition, LPS application remarkably increased the expression of p-IKK, while PAP pretreatment partly abolished this effect, which

indicated that PAP suppressed LPS-induced microglial activation probably by NF-κB signaling pathway.

Conclusion

In conclusion, we identified PAP not only suppressed the LPS-induced microglial activity by inhibiting transcription/ production of proinflammatory factors, but also promoted the transformation of activated BV2 cells from cytotoxic phenotypes (M1/M2b) to a neuroprotective phenotype (M2a). These effects were probably mediated by NF-κB signaling pathway. Therefore, we concluded PAP would be a promising candidate for the treatment of neurodegenerative diseases.

Acknowledgments

Author contributions

All authors contributed toward data analysis, drafting and critically revising the paper and agree to be accountable for all aspects of the work.

Disclosure

The authors report no conflicts of interest in this work.

References

1. Ellis-Behnke RG, Jonas RA, Jonas JB. The microglial system in the eye and brain in response to stimuli in vivo. *J Glaucoma*. 2013;22 (Suppl 5): S32–S35.
2. Nimmerjahn A, Kirchhoff F, Helmchen F. Resting microglial cells are highly dynamic surveillants of brain parenchyma in vivo. *Science*. 2005;308(5726):1314–1318.
3. Block ML, Zecca L, Hong JS. Microglia-mediated neurotoxicity: uncovering the molecular mechanisms. *Nat Rev Neurosci*. 200;8(1):57–69.
4. Gao HM, Hong JS. Why neurodegenerative diseases are progressive: uncontrolled inflammation drives disease progression. *Trends Immunol*. 2008;29(8):357–365.
5. Pocock JM, Liddle AC, Hooper C, Taylor DL, Davenport CM, Morgan SC. Activated microglia in Alzheimer's disease and stroke. *Ernst Schering Res Found Workshop*. 2002;(39):105–132.
6. Wang JW, Chen SD, Zhang XL, Jonas JB. Retinal microglia in glaucoma. *J Glaucoma*. Epub 2015 Feb 23. 7. Karlstetter M, Langmann T. Microglia in the aging retina. *Adv Exp Med Biol*. 2014;801:207–212.
8. Li HY, Ruan YW, Ren CR, Cui Q, So KF. Mechanisms of secondary degeneration after partial optic nerve transection. *Neural Regen Res*. 2014;9(6):565–574.
9. Zhang C, Lei B, Lam TT, et al. Neuroprotection of photoreceptors by minocycline in light-induced retinal degeneration. *Invest Ophthalmol Vis Sci*. 2004;45(8):2753–2759.
10. Dang Y, Xu Y, Wu W, et al. Tetrandrine suppresses lipopolysaccharide-induced microglial activation by inhibiting NF-κB and ERK signaling pathways in BV2 cells. *PLoS One*. 2014;9(8):e102522.
11. Li W, Yang C, Lu J, et al. Tetrandrine protects mouse retinal ganglion cells from ischemic injury. *Drug Des Devel Ther*. 2014;8:327–339.
12. Cho HK, Kee C. Population-based glaucoma prevalence studies in Asians. *Surv Ophthalmol*. 2014;59(4):434–447.
13. Howell GR, Libby RT, Jakobs TC, et al. Axons of retinal ganglion cells are insulted in the optic nerve early in DBA/2J glaucoma. *J Cell Biol*. 2007;179(7):1523–1537.
14. Neufeld AH. Microglia in the optic nerve head and the region of parapapillarychorioretinal atrophy in glaucoma. *Arch Ophthalmol*. 1999; 117(8):1050–1056.
15. Zhu W, Liu S, Zhao J, et al. Highly flexible and rapidly degradable papaverine-loaded electrospun fibrous membranes for preventing vasospasm and repairing vascular tissue. *Acta Biomater*. 2014;10(7): 3018–3028.
16. Kim JH, Yi HJ, Ko Y, et al. Effectiveness of papaverinecisternal irrigation for cerebral vasospasm after aneurysmal subarachnoid hemorrhage and measurement of biomarkers. *Neurol Sci*. 2014;35(5):715–722.
17. Yoshikawa M, Suzumura A, Tamaru T, Takayanagi T, Sawada M. Effects of phosphodiesterase inhibitors on cytokine production by microglia. *Mult Scler*. 1999;5(2):126–133.
18. Dang Y, Jiang Z, Zhu Y, Chiu K. Effects of papaverine on rat primary microglia. 2015. Submitted.
19. Tezel G, Li LY, Patil RV, Wax MB. TNF-alpha and TNF-alpha receptor-1 in the retina of normal and glaucomatous eyes. *Invest Ophthalmol Vis Sci*. 2001;42(8):1787–1794.
20. Yuan L, Neufeld AH. Tumor necrosis factor-alpha: a potentially neurodestructive cytokine produced by glia in the human glaucomatous optic nerve head. *Glia*. 2000;32(1):42–50.
21. Tezel G, Wax MB. Increased production of tumor necrosis factor-alpha by glial cells exposed to simulated ischemia or elevated hydrostatic pressure induces apoptosis in cocultured retinal ganglion cells. *J Neurosci*. 2000;20(23):8693–8700.
22. McCoy MK, Martinez TN, Ruhn KA, et al. Blocking soluble tumor necrosis factor signaling with dominant-negative tumor necrosis factor inhibitor attenuates loss of dopaminergic neurons in models of Parkinson's disease. *J Neurosci*. 2006;26(37):9365–9375.
23. Shohami E, Ginis I, Hallenbeck JM. Dual role of tumor necrosis factor alpha in brain injury. *Cytokine Growth Factor Rev*. 1999;10:119–130.
24. Su W, Li Z, Jia Y, Zhuo Y. Rapamycin is neuroprotective in a rat chronic hypertensive glaucoma model. *PLoS One*. 2014;9(6):e99719.
25. Yang F, Wu L, Guo X, Wang D, Li Y. Improved retinal ganglion cell survival through retinal microglia suppression by a chinese herb extract, triptolide, in the DBA/2J mouse model of glaucoma. *Ocul Immunol Inflamm*. 2013;21(5):378–389.
26. Mookherjee S, Banerjee D, Chakraborty S, et al. Association of IL1A and IL1B loci with primary open angle glaucoma. *BMC Med Genet*. 2010;11:99.
27. Maghzi AH, Minagar A. IL1-β expression in multiple sclerosis. *J Neurol Sci*. 2014;343(1–2):1.
28. Geller DA, de Vera ME, Russell DA, et al. A central role for IL-1 beta in the in vitro and in vivo regulation of hepatic inducible nitric oxide synthase. IL-1 beta induces hepatic nitric oxide synthesis. *J Immunol*. 1995; 155(10):4890–4898.
29. Schmid CD, Melchior B, Masek K, et al. Differential gene expression in LPS/IFNgamma activated microglia and macrophages: in vitro versus in vivo. *J Neurochem*. 2009;109(Suppl 1):117–125.
30. Lalancette-Hébert M, Gowing G, Simard A, Weng YC, Kriz J. Selective ablation of proliferating microglial cells exacerbates ischemic injury in the brain. *J Neurosci*. 2007;27(10):2596–2605.
31. Chhor V, Le Charpentier T, Lebon S, et al. Characterization of phenotype markers and neuronotoxic potential of polarised primary microglia in vitro. *Brain Behav Immun*. 2013;32(100):70–85.
32. Schafer P. Apremilast mechanism of action and application to psoriasis and psoriatic arthritis. *Biochem Pharmacol*. 2012;83(12):1583–1590.